Article

Cell Reports

Mycobacterial WhiB6 Differentially Regulates ESX-1 and the Dos Regulon to Modulate Granuloma Formation and Virulence in Zebrafish

Graphical Abstract

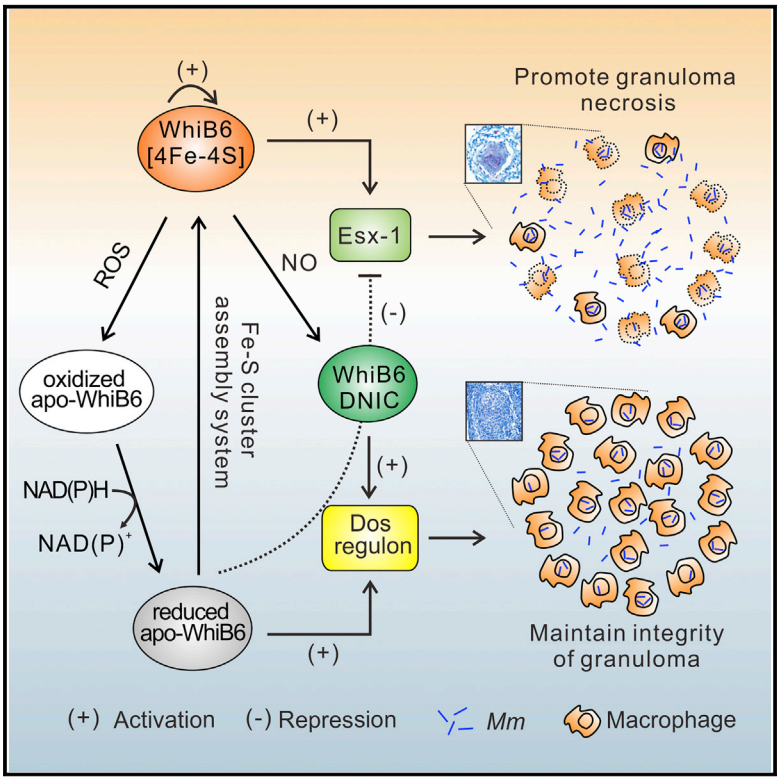

Highlights

- The WhiB6 Fe-S cluster is essential for ESX-1 function in *M. marinum*
- Disruption of the *M. marinum* WhiB6 Fe-S cluster modulates transcription in *M. marinum*
- WhiB6 dynamically regulates ESX-1 and DosR gene expression upon exposure to NO
- Isoforms of WhiB6 modulate *M. marinum* virulence and granuloma formation in zebrafish

Authors

Zhenkang Chen, Yangbo Hu, Bridgette M. Cumming, ..., Jiaoyu Deng, Adrie J.C. Steyn, Shiyun Chen

Correspondence

sychen@wh.iov.cn

In Brief

Chen et al. describe the cellular role of the WhiB6 protein in mycobacterial virulence, dissemination, sensing of extracellular stressors, and regulation of downstream genetic programs. WhiB6 regulation through its Fe-S cluster enables mycobacteria to establish persistent infection and maintain the integrity of granulomas.

Chen et al., 2016, Cell Reports *16*, 2512–2524
August 30, 2016
http://dx.doi.org/10.1016/j.celrep.2016.07.080

OPEN ACCESS
CellPress

Cell Reports
Article

Mycobacterial WhiB6 Differentially Regulates ESX-1 and the Dos Regulon to Modulate Granuloma Formation and Virulence in Zebrafish

Zhenkang Chen,[1,4] Yangbo Hu,[1] Bridgette M. Cumming,[2] Pei Lu,[1] Lipeng Feng,[1] Jiaoyu Deng,[1] Adrie J.C. Steyn,[2,3] and Shiyun Chen[1,5,*]

[1]Key Laboratory of Special Pathogens and Biosafety, Center for Emerging Infectious Diseases, Wuhan Institute of Virology, Chinese Academy of Sciences, Wuhan 430071, China
[2]KwaZulu-Natal Research Institute for Tuberculosis and HIV, Durban 4001, South Africa
[3]Department of Microbiology, University of Alabama at Birmingham, Birmingham, AL 35294, USA
[4]University of Chinese Academy of Sciences, Beijing 10086, China
[5]Lead Contact
*Correspondence: sychen@wh.iov.cn
http://dx.doi.org/10.1016/j.celrep.2016.07.080

SUMMARY

During the course of infection, *Mycobacterium tuberculosis* (*Mtb*) is exposed to diverse redox stresses that trigger metabolic and physiological changes. How these stressors are sensed and relayed to the *Mtb* transcriptional apparatus remains unclear. Here, we provide evidence that WhiB6 differentially regulates the ESX-1 and DosR regulons through its Fe-S cluster. When challenged with NO, WhiB6 continually activates expression of the DosR regulons but regulates ESX-1 expression through initial activation followed by gradual inhibition. Comparative transcriptomic analysis of the holo- and reduced apo-WhiB6 complemented strains confirms these results and also reveals that WhiB6 controls aerobic and anaerobic metabolism, cell division, and virulence. Using the *Mycobacterium marinum* zebrafish infection model, we find that holo- and apo-WhiB6 modulate levels of mycobacterial infection, granuloma formation, and dissemination. These findings provide fresh insight into the role of WhiB6 in mycobacterial infection, dissemination, and disease development.

INTRODUCTION

Mycobacterium tuberculosis (*Mtb*), the etiological agent of tuberculosis (TB), is one of the most successful intracellular pathogens. During infection, this pathogen is engulfed by resident (alveolar) macrophages and resides in the phagosome, whose environment has evolved to destroy invading agents (Flannagan et al., 2009). *Mtb* possesses a variety of mechanisms to survive within the phagosomal compartment or escape from it, ultimately leading to killing of the host cell (Ehrt and Schnappinger, 2009; Simeone et al., 2012). As infection progresses, infected macrophages recruit additional macrophages and other immune cells to form a granuloma, which is composed of mononuclear phagocytes, dendritic cells, and T and B lymphocytes (Philips and Ernst, 2012; Ramakrishnan, 2012).

It has been proposed that multiple stress factors inside the granuloma, such as NO, CO, low O_2, limited nutrients, and low pH, trigger *Mtb* to reprogram its metabolism to a non-replicating "dormant" state (Dutta and Karakousis, 2014; Schnappinger et al., 2003). The *Mtb* Dos dormancy regulon, consisting of the response regulator DosR and the heme-containing sensor kinases DosS and DosT, controls roughly 50 genes and is capable of responding to NO, CO, and hypoxia (Kumar et al., 2007, 2008; Shiloh et al., 2008; Voskuil et al., 2003). Studies have shown that the Dos dormancy regulon maintains energy levels and redox balance (Leistikow et al., 2010; Rustad et al., 2009). It is also believed that the Dos regulon is essential for *Mtb* to persist in lung lesions (Boon and Dick, 2012). WhiB5 has been characterized as a transcriptional regulator that controls the expression of genes involved in *Mtb* reactivation (Casonato et al., 2012). However, the genetic mechanism whereby *Mtb* enters, maintains, and emerges from a dormant state is poorly understood.

Recent studies have made progress in understanding how *Mtb* senses redox signals such as O_2 and NO via the family of Fe-S cluster-containing WhiB proteins in addition to the heme-based DosR/S/T system. Members of the WhiB family of redox sensor proteins exert diverse functions, including cell division (WhiB2), fatty acid metabolism and pathogenesis (WhiB3), and antibiotic resistance (WhiB7) (Burian et al., 2013; Konar et al., 2012; Singh et al., 2007, 2009). However, the mechanisms whereby these proteins sense and respond to signals to exert their regulatory effects are largely unknown. Noticeably, *whiB6* expression is highly induced upon treatment with NO and upregulated during infection of macrophages (Larsson et al., 2012; Saini et al., 2012a, 2012b). In another genome-wide expression study, *whiB6* (Rv3862c) expression was upregulated under prolonged hypoxia (Homolka et al., 2010). Using an ELISA, WhiB6 was detected as a reactivation-associated antigen in active TB patients to stimulate interferon-γ (IFN-γ) (Kassa et al., 2012).

Recently, chromatin immunoprecipitation sequencing (ChIP-seq) with high-resolution transcriptomic analyses has shown that PhoP controls ESX-1 via EspR (Solans et al., 2014b). Furthermore, comparative gene expression analysis between *Mtb* H37Rv and numerous clinical isolates has demonstrated that single-nucleotide insertion in the promoter region of *whiB6* in *Mtb* H37Rv has changed the regulatory role of PhoP on WhiB6, which was identified as a novel ESX-1 component (Solans et al., 2014a).

The ESX-1 locus encodes a type VII secretion system, which is necessary for virulence and is highly conserved in both *Mtb* and *Mycobacterium marinum* (*Mm*) (Joshi et al., 2012; McLaughlin et al., 2007), a genetically close relative of *Mtb*. ESX-1 is an extensively studied genetic locus involved in mycobacterial dissemination and granuloma formation as demonstrated by the zebrafish embryo model (Davis and Ramakrishnan, 2009). The 6-kDa early-secreted antigenic target (ESAT-6), a well-known virulence factor, is secreted via the ESX-1 secretion system (Champion et al., 2014; Volkman et al., 2004). Several roles have been attributed to ESAT-6, which is a membrane lytic factor that enables phagosomal escape, suggesting that ESX-1-mediated translocation from the phagolysosome to the macrophage cytoplasm in both species is a central virulence mechanism of pathogenic mycobacteria (Abdallah et al., 2011; Houben et al., 2012).

Here, we hypothesize that *Mm* WhiB6 plays a role in virulence. To test this hypothesis, we examined the expression profiles of an *Mm whiB6* mutant and performed complementation studies with *Mtb whiB6*. Importantly, we have shown that WhiB6 plays a role in regulating the ESX-1 secretion system and the Dos dormancy regulon. We have examined the mechanism of regulation by making use of WhiB6 Fe-S cluster mutants and studying the effect of NO on ESX-1 and Dos expression. Lastly, we examined the dissemination of *Mm* with mutated alleles of *whiB6* in the zebrafish model for TB. It is anticipated that these findings will provide fresh insight into the role of WhiB6 in granuloma formation and virulence.

RESULTS

WhiB6 Regulates the Expression of Genes Associated with the ESX-1 Secretion System

MMAR_5437 in *Mm* (homologous to *whiB6* in *Mtb*) is conservatively located adjacent to the ESX-1 genetic locus. Alignment of the ESX-1 gene cluster in *Mm* and *Mtb* revealed that both open reading frame (ORF) sequences and genomic organizations are highly conserved (Figure 1A). We therefore asked if WhiB6 regulates expression of genes belonging to the ESX-1 system.

First, *Mm whiB6* was replaced by a hygromycin resistance cassette (Figure S1A) to generate the *Mm whiB6* mutant (Δ*whiB6*), which was confirmed by Southern blot (Figure S1B). Next, an episomal plasmid (pMV261) and an integrated plasmid (pMV306), both without the *hsp60* promoter, expressing either *Mm whiB6* ($whiB6_M$) or *Mtb* CDC1551 *whiB6* ($whiB6_T$) under the control of their native promoters, were introduced into Δ*whiB6*, generating pMV261-MB6/Δ*whiB6* (MB6) and pMV261-TB6/Δ*whiB6* (TB6) and pMV306-MB6 and pMV306-TB6, respectively. Expression of $whiB6_M$ was subsequently tested by qRT-PCR (Figure S2A).

The expression of several ESX-1 genes (*pe35*, *espE*, *esxA*, and *esxB*) in the complemented strains was analyzed by qRT-PCR. As shown in Figure 1B, transcription of ESX-1-associated genes was significantly reduced in Δ*whiB6*. On the contrary, induction of these genes was significantly higher in MB6 than in Δ*whiB6* harboring the empty vector (Δ*whiB6*-vec). Similar results were also obtained from pMV306-MB6 and pMV306-TB6 complemented strains (Figures 1B and S2C). In addition, MB6 was able to substantially boost ESAT-6 secretion compared to Δ*whiB6*-vec (Figure S2B).

To further investigate whether WhiB6 regulates the ESX-1 genetic locus, chromatin immunoprecipitation (ChIP) experiments were performed using polyclonal antibodies against WhiB6. The data showed that the promoter regions of *espA*, *whiB6*, *espE*, *and eccA1* genes were significantly enriched in *Mm* wild-type (WT) and MB6 strains compared to their respective mutant strains (Figure 1C). The differences observed in the promoter binding activities between the WT and MB6 strains could be as a result of WhiB6 being more highly expressed in MB6, which may have resulted in imbalances in antigen-antibody ratios and precipitation during ChIP processing. To further analyze whether WhiB6 autoregulates itself, WT and Δ*whiB6* were transformed with either pMV261 harboring native *whiB6* promoters from *Mm*, *Mtb* H37Rv, or *Mtb* CDC1551 strains that were translationally fused with the *egfp* reporter gene. Fluorescence quantification demonstrated that autoregulation of *whiB6* occurs in both *Mm* and *Mtb* CDC1551, but not in *Mtb* H37Rv (Figure 1D). This result was further confirmed by western blotting and qRT-PCR in *Mm* (Figure 1E). As observed in a recent study (Solans et al., 2014a), a specific polymorphism in H37Rv, a G insertion at the −74 position upstream of *whiB6* start codon, significantly reduced the promoter activity of *whiB6* compared to that of CDC1551 in WT, but this difference was abolished in Δ*whiB6* (Figure 1D).

In sum, these data demonstrate that WhiB6 regulates the expression of several genes belonging to the ESX-1 secretion system. Further analyses have shown that WhiB6 is conserved in *Mtb* and *Mm*.

The WhiB6 Fe-S Cluster Is Essential for ESX-1 Function

Here, we investigated the role of the WhiB6 Fe-S cluster in regulating the ESX-1 secretion system. Alignment of the *Mm* and *Mtb* WhiB6 protein sequences shows high similarity (Figure 2A). The four conserved Cys residues in WhiB6 (i.e., Cys-14, 33, 36, αvδ 42 in *Mm* and Cys-34, 53, 56, and 62 in *Mtb*) are conserved among the WhiB family (Figure 2B). To analyze the role of these conserved Cys residues in WhiB6, the Cys residues were mutated to Ser, and these mutants were assessed by measuring the hemolysis of sheep red blood cells (sRBC) in a contact-dependent and ESX-1-dependent manner. An in vitro hemolysis assay suggested that ESX-1, which is regulated by WhiB6, is fully responsible for hemolysis (Gao et al., 2004), as ESX-1 formed pores in the cell membrane. As seen in Figure 2C, Δ*whiB6* showed markedly reduced hemolytic activity compared to WT, whereas MB6 and TB6 completely restored hemolytic activity. Noticeably, all the mycobacteria with mutated Cys alleles showed significantly decreased hemolytic activity (Figure 2C). Consistent with this result, decreased levels of ESAT-6 (EsxA) and CFP-10 (EsxB) were detected in the culture filtrate of

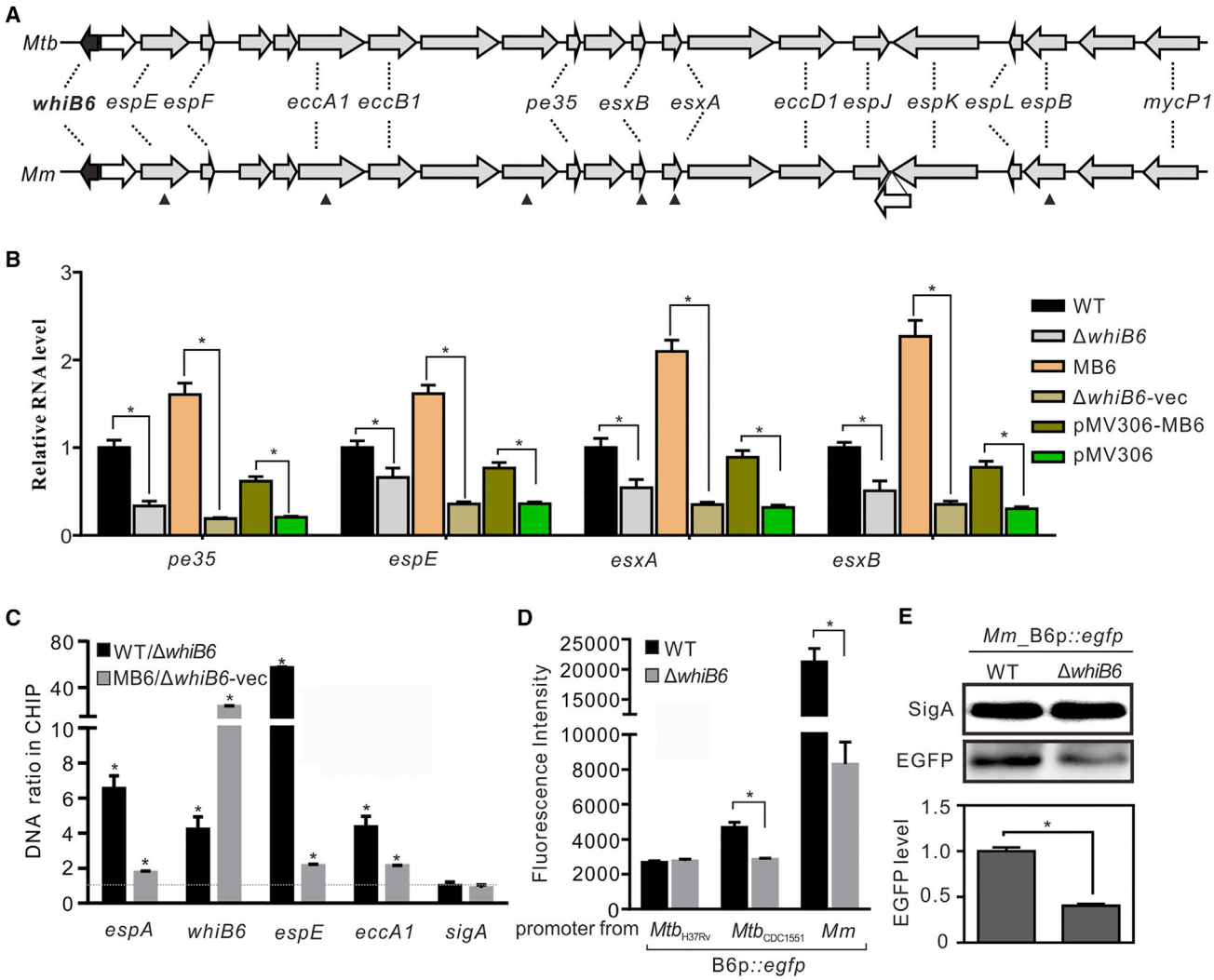

Figure 1. WhiB6 Regulates ESX-1-Associated Gene Expression

(A) Alignment of ESX-1 and its extended genes in *Mm* and *Mtb*. Triangles indicate genes that were selected for further analysis of ESX-1 expression.

(B) qRT-PCR analysis of mRNA levels of *pe35*, *espE*, *esxA*, and *esxB* in *Mm* strains as indicated.

(C) ChIP-qPCR enrichment for binding of WhiB6 to the promoter regions of *espA*, *whiB6*, *espE*, and *eccA1* in WT/Δ*whiB6* or MB6/Δ*whiB6*-vec. The enrichment for binding of WhiB6 to the coding region of *sigA* in these strains was used as a negative control.

(D) Fluorescence intensity of EGFP in WT and Δ*whiB6*, which was introduced with pMV261 harboring native promoters of either *whiB6* from *Mtb* H37Rv, *Mtb* CDC1551, or *Mm* strains, respectively, and translationally fused with *egfp*.

(E) Western blot (top) and qRT-PCR (bottom) of WT and Δ*whiB6* transformed with pMV261 harboring native promoters of MB6 fused with *egfp*.

Statistical significance was determined by Student's t test (B–E) and displayed as *p < 0.05 in the comparisons as indicated. Data are representative of three independent experiments (B, D, and E) or two qRT-PCR experiments (C).

Δ*whiB6* (Figure 2D), whereas complementation in TB6 and MB6 restored secretion of EsxA and EsxB (Figure 2D) in the culture filtrate. Although EsxA and EsxB in the pellet fractions of Δ*whiB6* and WT were comparable, EsxA and EsxB levels were reduced in the culture filtrate of *ΔwhiB6* relative to the WT. In contrast, introduction of any one of the Cys mutant alleles (named TB6-C34S or MB6-C14S) or all four Cys mutant alleles (named TB6-4CS or MB6-4CS) led to reduced levels of EsxA and EsxB in the pellet and culture filtrate (Figure 2D).

These findings are consistent with the gene expression findings in Figures 2E and 2F where the C14S and 4CS mutated alleles of MB6, and the C34S and 4CS mutated alleles of TB6, failed to restore expression of ESX-1-associated genes (see also Figures S2C and S3A–S3D). Altogether, these results strongly suggest that an intact Fe-S cluster in both *Mm* WhiB6 and *Mtb* WhiB6 is essential for the regulation of ESX-1.

Disruption of the Fe-S Cluster of WhiB6 Modulates the Transcriptional Profile in *Mm*

We noticed that mutating the four conserved Cys residues to Ser in *Mm* WhiB6 and *Mtb* WhiB6 induced faster growth rates (Figure S5A). In addition, using UV-visible absorption

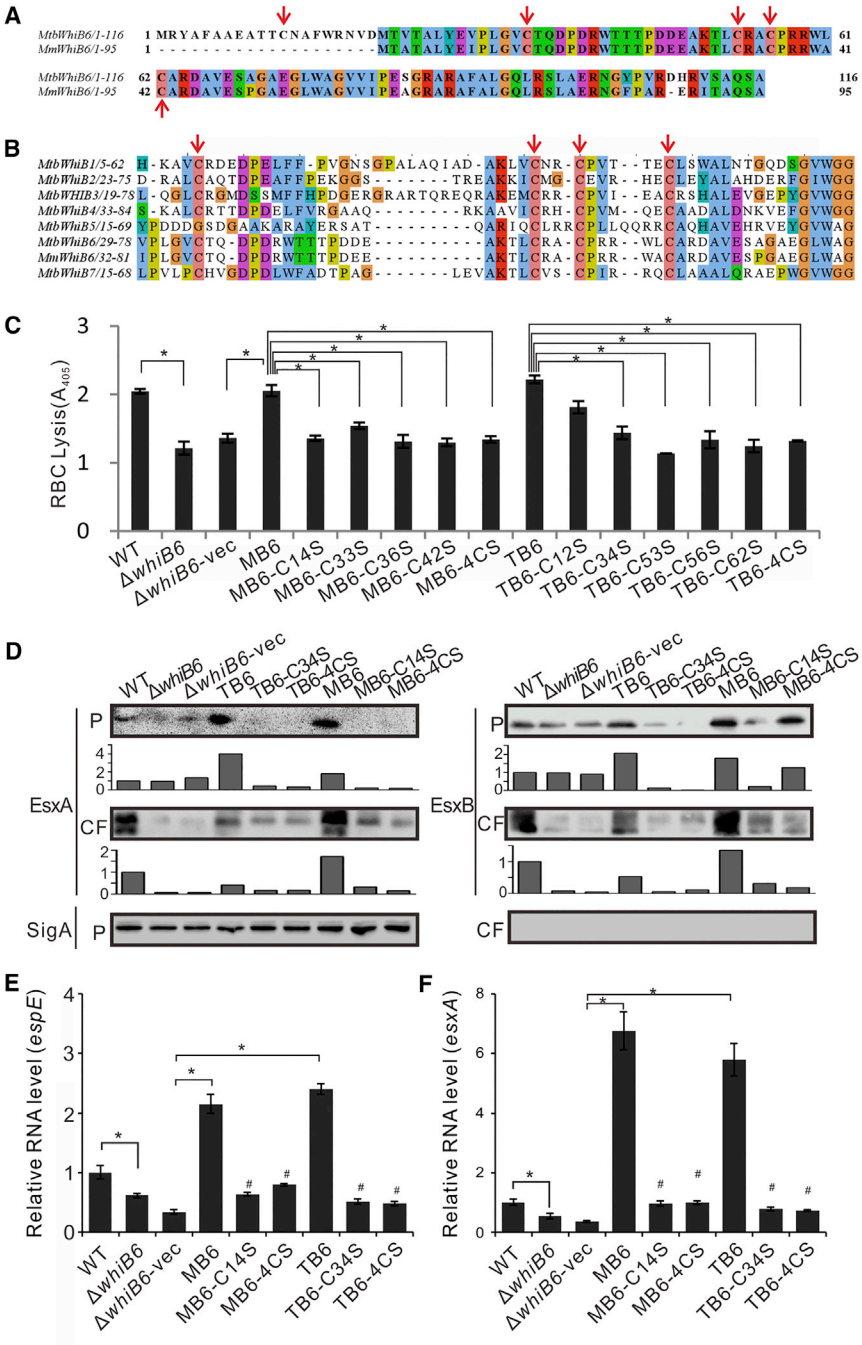

Figure 2. Intact Fe-S Clusters in WhiB6 Are Essential for the Function of ESX-1

(A) Sequence alignment of WhiB6 from *Mtb* and *Mm*. The four conserved cysteines are highlighted in pink. Residues mutated in this study are indicated with red arrows.

(B) Sequence alignment of WhiB family proteins. The four conserved cysteines are highlighted in pink and indicated by red arrows.

(C) Mutation of cysteine to serine in WhiB6 alters ESX-1 function as observed by the hemolytic activities of the different *Mm* strains on sheep RBCs.

(D) Western blot analysis of EsxA (ESAT-6) and EsxB (CFP-10) in the whole cell (P) and culture filtrate (CF) of indicated *Mm* strains. SigA was used as a control of bacterial integrity in each sample. Signal intensity was quantified, standardized to the intensity of SigA in the pellet, and plotted below the western blot images.

(E and F) qRT-PCR analysis of mRNA levels of *espE* (E) and *esxA* (F).

Data are representative of three (C, E, and F) or two (D) experiments. Statistical significance is displayed as $^{*}p < 0.05$ using one-way ANOVA with Tukey's post-test for multiple comparisons (C, E, and F) and $^{\#}p < 0.05$ compared with their respective complementation strains (MB6 or TB6).

spectroscopy, we observed an increase in yellow pigment color with a peak at ~430–450 nm in the culture supernatants of MB6-4CS and TB6-4CS compared to that of MB6 and TB6 (Figures S5B–S5D). Therefore, we hypothesized that the WhiB6 Fe-S cluster is an essential prosthetic group that regulates a diverse set of genes including the ESX-1 secretion system. To test this hypothesis, transcriptomic profiling was performed on MB6, MB6-4CS, and Δ*whiB6*-vec strains. Relative to Δ*whiB6*-vec, ESX-1-associated genes were upregulated in MB6, but not in MB6-4CS, in which *espACD* (*espA-MMAR4167-MMAR4168*) and *esxAB* expression was significantly reduced (Figure S6A).

To explain why MB6 and MB6-4CS exhibit distinct growth phenotypes, expression of genes that participate in energy metabolism (notably the electron transport chain and ATP synthase) was examined (Figure 3A). Significant downregulation of genes encoding the components of the cytochrome *c* pathway in the electron transport chain bc1 complex (*qcrCAB*), aa3-type cytochrome *c* oxidase (*ctaBCDE*), and cytochrome bd (*cydABCD*) were observed in MB6. Similar results were also observed in genes encoding components of F_0F_1 ATP synthase. In contrast, most of these genes are upregulated in MB6-4CS compared to the vector control (Figure 3A). In addition, genes related to cell division, including *ftsK* and *xerC*, which are involved in chromosome segregation (Goodsmith et al., 2015), were similarly expressed in Δ*whiB6*-vec and MB6 strains but highly expressed in MB6-4CS. Interestingly, expression of genes related to the cell wall biosynthetic gene operons (*murE-ftsQ*, *pimAB*, and *embCAB*) was significantly downregulated in MB6, but most returned to similar levels in MB6-4CS (Figure 3A).

Unexpectedly, introduction of MB6-4CS into Δ*whiB6* mimics a hypoxic response. This was demonstrated by the fact that

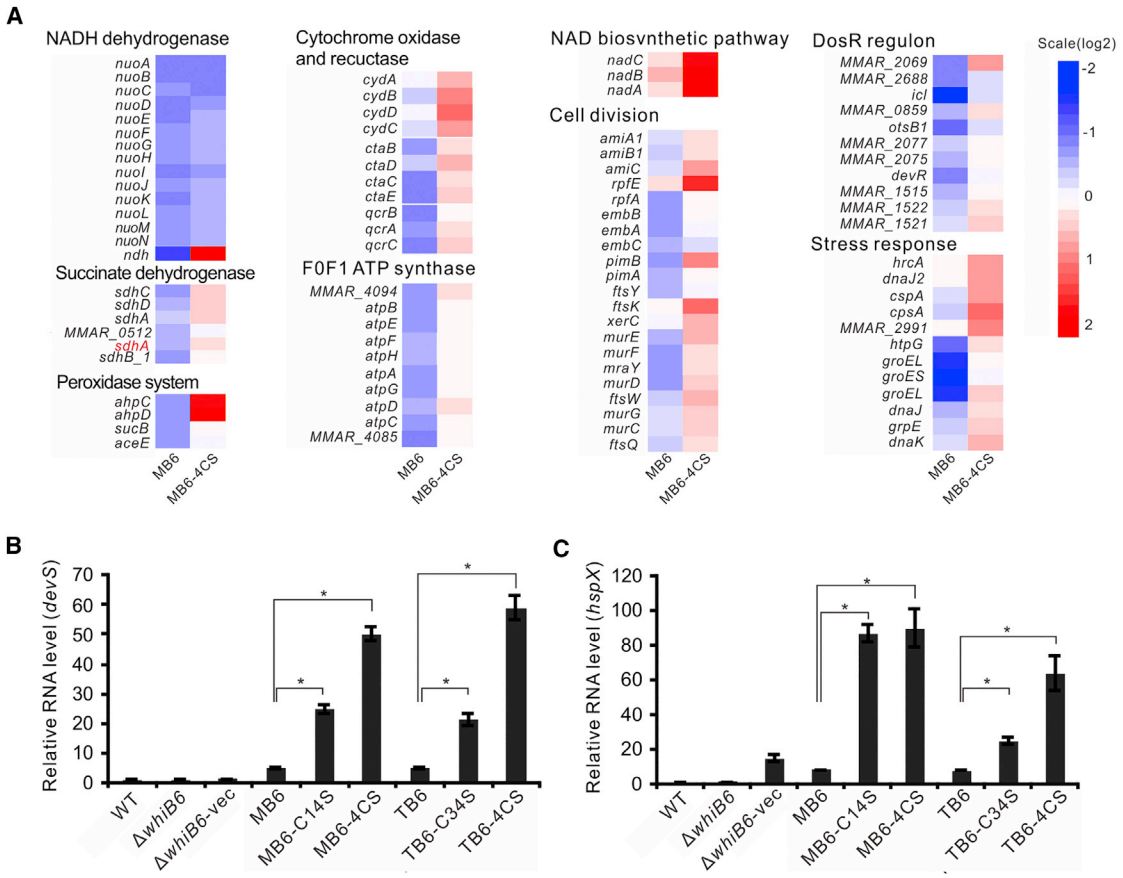

Figure 3. Holo- and Apo-WhiB6 Differentially Regulate Gene Expression

(A) WhiB6 modulates the expression of energy metabolism and cell division related genes. Average expression values from two independent experiments in MB6 and MB6-4CS strains were divided by that in Δ*whiB6*-vec. Genes with statistically significant changes in expression were determined by two-tailed, unpaired Student's t test (1.5-fold up- and downregulated, $p < 0.05$). *sdhA* in red is *MMAR_0511* and *sdhA* in black is *MMAR_1201*.

(B and C) qRT-PCR analysis of dormancy related genes. Statistical significance was determined by one-way ANOVA with Tukey's post-test for multiple comparisons and displayed as *$p < 0.05$. Data are representative of three experiments (B and C).

MB6-4CS, which is similar to reduced apo-WhiB6, significantly induced the de novo NAD(P) biosynthetic pathway-related gene *ndh*, as well as the stress-induced chaperone genes, *sdh-1* (*MMAR_0512-sdhB_1*) and *sdh-2* (*sdhC-sdhA*), and also the dormancy-related regulon (Boshoff et al., 2008; Hartman et al., 2014; Voskuil et al., 2003). These genes were all significantly downregulated in MB6 compared to Δ*whiB6*-vec (Figure 3A). Two types of NADH dehydrogenases are found in mycobacteria, type I encoded by *nuoA-N* and type II encoded by *ndh*. NDH-1 is utilized during aerobic respiration and the acute stage of infection, while NDH-2 is induced during anaerobic electron transfer (Rao et al., 2008). Only *ndh* was upregulated in MB6-4CS compared to MB6, but not *nuoA-N*, whose mRNA level is comparable among MB6 and MB6-4CS strains (Figure 3A). Thus, disruption of the WhiB6 Fe-S cluster mimics hypoxic conditions that shift metabolism away from oxygen consumption and induce the dormancy regulon to maintain ATP levels and balance the redox state.

Importantly, the Dos dormancy genes (i.e., *devH (mmar_1515)-devR-devS* operon), as well as *hspX* and *tgs1* genes, were all significantly induced in MB6-C14S and MB6-4CS relative to MB6 as confirmed by qRT-PCR (Figure 3B; see also Figures S3E and S3F). Similar results were also observed in the TB6-C34S and TB6-4CS strains. UV-visible spectra revealed that single serine mutants in both MB6-C14S and TB6-C34S still have Fe-S clusters, which was abolished in MB6-4CS and TB6-4CS (Figures S4A and S4B), suggesting that a single serine mutant with the Fe-S cluster may have changed their physiochemical states compared to that of wild-type WhiB6 (Hurley et al., 1997).

In sum, these findings point to a prosthetic switching mechanism whereby the WhiB6 Fe-S cluster functions independently of apo-WhiB6 to regulate gene expression. More specifically, our transcriptomic data show that the WhiB6 Fe-S cluster is necessary for the negative control of the *dosR* regulon and positive control of the ESX-1 secretion system, whereas apo-WhiB6 induces the *dosR* regulon and suppresses ESX-1 expression. These findings have important implications for understanding the mechanisms of mycobacterial virulence.

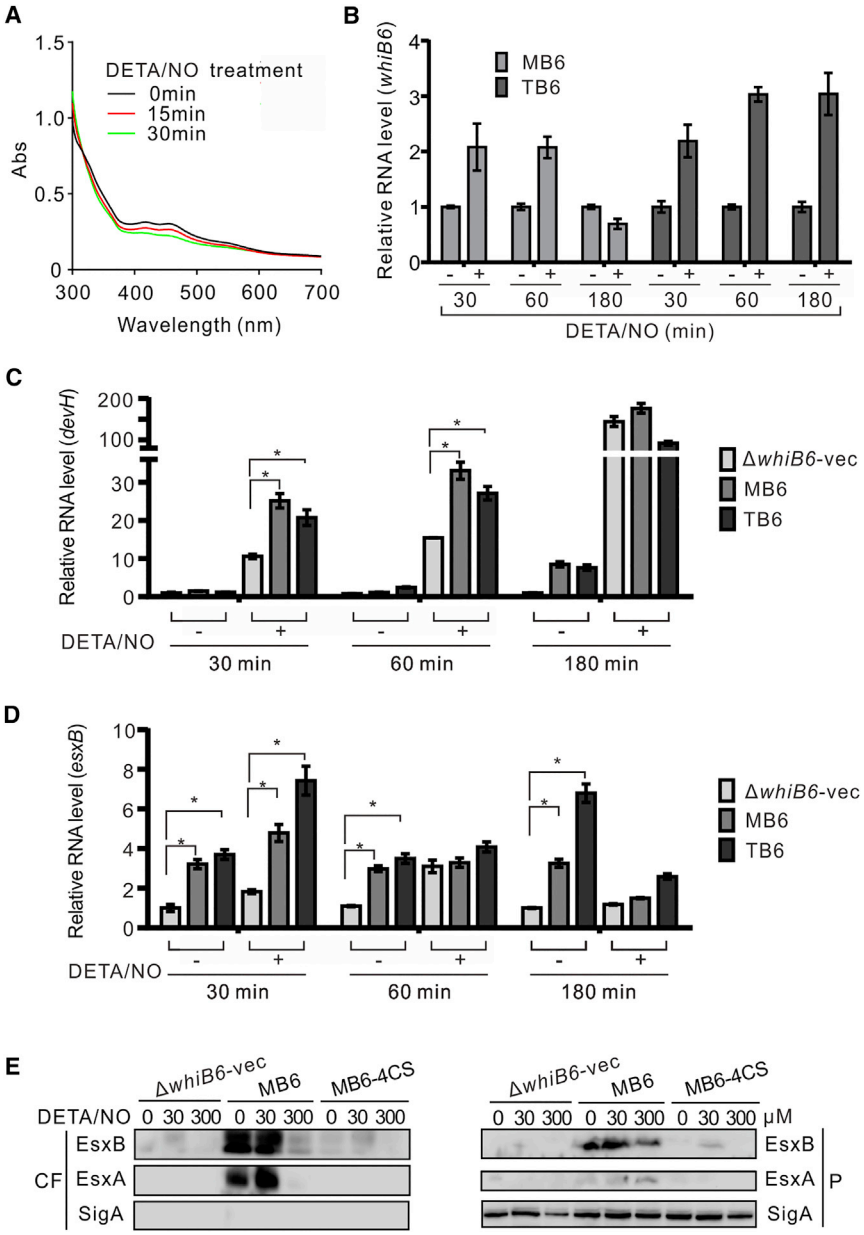

Figure 4. WhiB6 Regulates ESX-1 and the Dormancy Regulon on Exposure to NO

(A) UV-visible spectra of anaerobically purified WhiB6 before and after exposure to 5 mM DETA-NO at the indicated time points.

(B) Relative expression levels of *whiB6* in the indicated *Mm* strains following exposure to 300 μM DETA-NO for 30, 60, and 180 min.

(C) Relative expression levels of *devH* when *Mm* complemented strains were exposed to 300 μM DETA-NO at the indicated time points.

(D) Relative expression levels of *esxB* when exposed to 300 μM DETA-NO at the indicated time points.

(E) Western blot analysis of expression and secretion of ESAT-6 (EsxA) and CFP-10 (EsxB) when *Mm* complemented strains were challenged with 0, 30, and 300 μM DETA-NO for 12 hr.

Statistical significance was determined by one-way ANOVA with Tukey's post-test for multiple comparisons and displayed as *$p < 0.05$. Data are representative of two experiments.

WhiB6 Reacts with NO to Dynamically Regulate the ESX-1 and Dos Dormancy Genes

Given that WhiB6 expression is highly induced upon treatment with NO (Geiman et al., 2006), we tested the hypothesis that NO binds to the WhiB6 Fe-S cluster to regulate expression of ESX-1 and the *dosR* regulon. NO is a key component of the innate immune response to mycobacterial infection and can react with the WhiB Fe-S clusters, resulting in the formation of a dinitrosyl-iron dithiol complex (DNIC) (Singh et al., 2007; Spiro, 2007). Therefore, anaerobically purified WhiB6 was treated with the NO-releasing compound diethylenetriamine nitric oxide (DETA-NO) under anaerobic conditions, and the response of the Fe-S cluster was monitored by UV-visible spectroscopy at different time points. As shown in Figure 4A, addition of DETA-NO resulted in decreased absorbance at 420 nm/480 nm and increased absorbance at ~300–320 nm, indicative of the formation of DNICs (Chawla et al., 2012). Thus, like most WhiB family proteins, WhiB6 also reacts with NO to form a nitrosylated Fe-S cluster.

In order to investigate the effects of nitrosylated WhiB6 on ESX-1 and DosR expression, MB6, TB6, and Δ*whiB6*-vec strains were challenged with DETA-NO at various time points to mimic conditions in activated macrophages. Time-course studies showed that $whiB6_T$ expression was induced under NO exposure in a time-dependent manner (Figure 4B). Expression of $whiB6_M$ was also induced during NO exposure, while its mRNA levels were gradually reduced after 60-min NO exposure (Figure 4B). Transcription of *devH*, the first gene of the *devH-devR-devS* operon, was increased in a time-dependent manner in MB6 and TB6 in comparison to Δ*whiB6*-vec when challenged with DETA-NO (Figure 4C). However, this differential expression was diminished after 3 hr (Figure 4C), pointing toward a complex interaction of NO with the WhiB6 and DosR regulons.

Given that the first gene of the *esxB-esxA* operon, *esxB* was evaluated to determine the role of WhiB6 in the ESX-1 secretion system. As seen in Figure 4D, *esxB* gene expression was highly induced after 30-min NO exposure in TB6 and MB6 but rapidly decreased until 60 min postexposure. Interestingly, activation of *esxB* was significantly reduced in TB6 and MB6 strains after 3-hr NO exposure (Figure 4D). Notably, secretion of EsxA and EsxB was significantly decreased when MB6 was exposed to

300 μM DETA-NO, demonstrating NO-induced downregulation of the ESX-1 secretion system (Figure 4E). Our previous results (Figure 2) also confirmed that the intact Fe-S cluster of WhiB6 acts as a positive regulator for ESX-1. These results further confirmed that WhiB6 differentially regulates ESX-1 and the Dos regulon by Fe-S cluster sensing of NO.

Isoforms of WhiB6 Modulate Virulence of *Mm* and Granuloma Formation in Zebrafish

Based on the above data, we hypothesize that WhiB6 participates in granuloma formation. To confirm this, the virulence of the *Mm* strains was first assessed by calculating the survival rates of intraperitoneally infected adult zebrafish at a high dosage (~5,000 cfu). As seen in Figure 5A, fish infected with MB6 and TB6 complemented strains exhibited high mortality (endpoint mortality ~80%), whereas fish infected with MB6-4CS and TB6-4CS showed increased survival (endpoint mortality ~20%). Zebrafish infected with WT, Δ*whiB6*, and Δ*whiB6*-vec had similar survival rates (~40%–50%).

Subsequently, to determine whether disease severity caused by MB6 and MB6-4CS correlates with granuloma necrosis in zebrafish (Cambier et al., 2014), the kinetics of granuloma formation in these strains was assessed. At 2 weeks post-infection (wpi), macrophage aggregates and organized granulomas occurred throughout the body in both WT and Δ*whiB6* infection groups (Figures 5B and 5D). At 4 wpi, granulomas were more abundant but less uniformly organized with multicentric necrotic areas in zebrafish infected with Δ*whiB6* compared to the WT infection group (Figures 5C and 5E). MB6 and TB6 accelerated necrosis and disruption of granulomas accompanied by patches of bacteria that appeared to be outside the granulomas (Figures 5G and 5J). In contrast, the vector control showed well-organized and centrally necrotized granulomas as well as fewer bacteria outside the granulomas (Figure 5F). However, when zebrafish were infected with MB6-4CS and TB6-4CS, less granuloma formation was observed, with little evidence of necrosis (Figures 5H and 5K). At 4 wpi, MB6-4CS and TB6-4CS also formed well-organized granulomas, where acid-fast-stained mycobacteria still resided (Figures 5I and 5L). Our results suggest that WhiB6 modulates not only mycobacterial virulence but also the duration of necrotic granuloma formation.

Because granuloma necrosis is closely related to extracellular granuloma growth of *Mm* (Pagán and Ramakrishnan, 2014; Tobin et al., 2010), we therefore examined replication and dissemination of *Mm* strains complemented with WT and mutated *whiB6* in zebrafish larvae, which lack functional lymphocytes (Langenau and Zon, 2005). As expected, although all groups had comparable bacterial burdens at 1 day postinfection (dpi), *whiB6* complementation groups had higher bacterial burdens and dispersed more rapidly to the head compared to their respective mutant allele complementation groups 4 dpi (Figures 6A and 6B; see also Figures S7A–S7D). At 7 dpi, bacterial burdens were exacerbated in the MB6- and TB6-infected zebrafish, resulting in clear local tissue damage, whereas fewer bacteria were observed in the head of zebrafish larvae infected with TB6-4CS and MB6-4CS strains (Figures S7E–S7H).

To assess whether co-infection of MB6 with MB6-4CS and Δ*whiB6*-vec could increase bacterial survival and dissemination to the head by caudal infection, the three genotypes were paired with each other for further assessment. At 4 dpi, in groups co-infected with the MB6 strain, resident bacteria were observed in the head of all zebrafish larvae (Figures 6C and 6D). In contrast, almost 50% fewer larvae simultaneously infected with MB6-4CS and Δ*whiB6*-vec strains had bacteria in the head at 4 dpi, but not at 7 dpi, in which 100% of all larvae groups had head infection (Figure 6D). However, when fluorescence of the bacterial burdens was measured for these groups at 7 dpi, a significant reduction in fluorescence was observed in the group co-infected with MB6-4CS and Δ*whiB6*-vec compared to the other two groups (Figure 6E). Thus, these findings suggest that isoforms of WhiB6 levels modulate virulence and granuloma formation as well as replication and dissemination of *Mm* in zebrafish.

DISCUSSION

Identification and characterization of genes necessary for persistence in vivo will provide insight into bacterial biology and host defense strategies (Goodsmith et al., 2015). *Mtb* resists elimination by the host immune system by detoxification of reactive oxygen and reactive nitrogen molecules such as NO produced by the host (Ehrt and Schnappinger, 2009). However, the molecular mechanisms underlying these processes still need to be addressed (Gengenbacher and Kaufmann, 2012). As suggested, future *Mtb* studies need to focus on protein functions in conditions mimicking the in vivo environment of *Mtb* infection (Cumming and Steyn, 2015). Seven WhiB family proteins are associated with developmental processes in *Mtb*. These proteins have been documented to be DNA-binding proteins in vitro, but the relationship between their regulatory roles and important properties of Fe-S cluster-based WhiB proteins sensing O_2 and NO are still unclear.

As part of the PhoP regulon, WhiB6 was found to regulate ESX-1 expression (Solans et al., 2014a), but the regulatory mechanism remains unknown. Our in vivo studies demonstrate that, similar to one WhiB-like protein (Wbl) (Smith et al., 2010), WhiB6 utilizes its transient forms to participate in the regulatory process of ESX-1-related genes. Disruption of intact Fe-S clusters in WhiB6 of both *Mtb* and *Mm*, which occurs upon continuous exposure to O_2 (Alam et al., 2009), abolishes their activation of the expression and secretion of ESX-1, further demonstrating conservation of WhiB6 and ESX-1 between *Mtb* and *Mm* in terms of function. In addition, autoregulation of WhiB6 in *Mtb* H37Rv was abolished due to a sole G inserted at the −74 position relative to the *Mtb* CDC1551 *whiB6* start codon, contributing to the explanation that clinical isolates of *Mtb* produce and secrete larger amounts of ESAT-6 than the widely used *Mtb* H37Rv laboratory strain (Solans et al., 2014a). Interestingly, while $whiB6_T$ was able to complement the ESX-1 system for secretion in *Mm*, relatively low levels of ESX-1 substrates were expressed in the TB6 strain.

The success of *Mtb* infection is based on the reprogramming of macrophages after primary infection/phagocytosis to prevent its own destruction. The ESX-1 virulence locus enables mycobacteria to escape from the microbiocidal phagosome of the macrophage, where the largest source of oxidative stress is present. Inducible NO synthase (iNOS/NOS2) is expressed in *Mtb*-infected macrophages, leading to the generation of NO

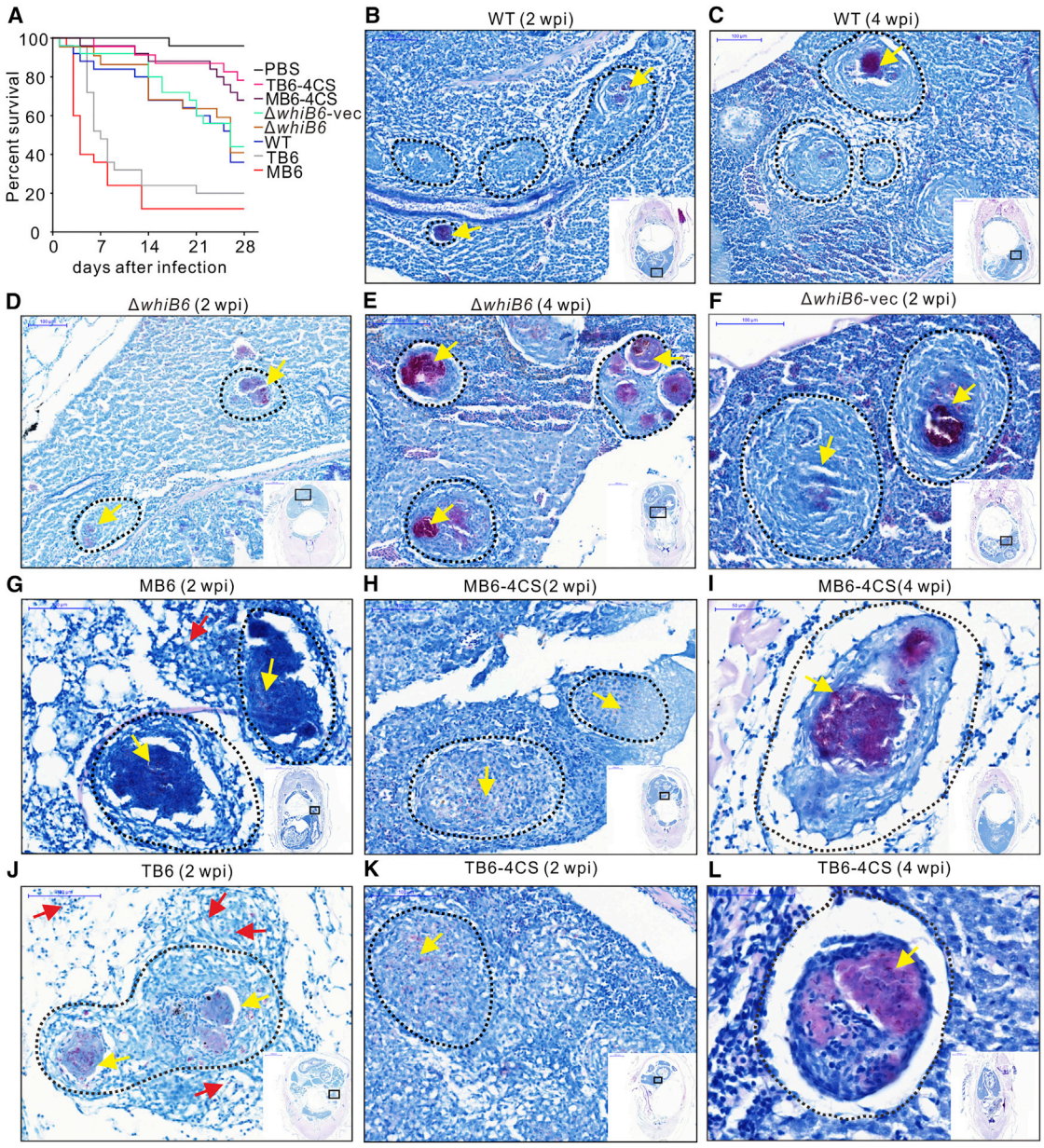

Figure 5. Holo- and Reduced Apo-WhiB6 Modulate Virulence of *Mm* and Granuloma Necrosis in Adult Zebrafish

(A) Kaplan-Meier graph showing survival of adult zebrafish injected intraperitoneally with ~5,000 cfu the indicated *Mm* strains or an equivalent volume of PBS. n = 25 for each group. Survival was compared by log-rank test: MB6 versus Δ*whiB6*-vec, MB6 versus MB6-4CS, and TB6 versus TB6-4CS, $p < 0.0001$; TB6 versus Δ*whiB6*-vec, $p < 0.001$; TB6-4CS versus Δ*whiB6*-vec, $p < 0.05$; MB6-4CS versus Δ*whiB6*-vec,$p = 0.0727$; and WT versus Δ*whiB6*, $p = 0.6633$.

(B–E) Representative Ziehl-Neelsen stains of adult zebrafish infected with WT (B and C) or Δ*whiB6* (D and E) at 2 weeks (B and D) or 4 weeks (C and E) after infection, respectively. Scale bars, 100 μm.

(F–H, J, and K) Representative Ziehl-Neelsen stains of adult zebrafish 2 weeks postinfection with *Mm* strains. Scale bars, 100 μm.

(I and L) Representative Ziehl-Neelsen stains of adult zebrafish 4 weeks postinfection with MB6-4CS (I) and TB6-4CS (L). Scale bars, 50 μm. Dotted circles delineate granulomas.

Yellow arrows indicate mycobacteria inside granulomas, and red arrows indicate mycobacteria outside granulomas. Three fish per group were used for each time point.

(Chan et al., 1995; Chan et al., 1992). When challenged with NO, WhiB6 dynamically regulates the expression of ESX-1 by initial activation followed by gradual inhibition of ESX-1. Our in vitro data indicate that WhiB6 directly reacts with NO, which suggests that WhiB6-DNIC potentially downregulates ESX-1 (Figure 4). Thus, our results provide convincing evidence that WhiB6 responds to nitrosative/oxidative stresses encountered within the macrophage, thereby differentially modulating the function of

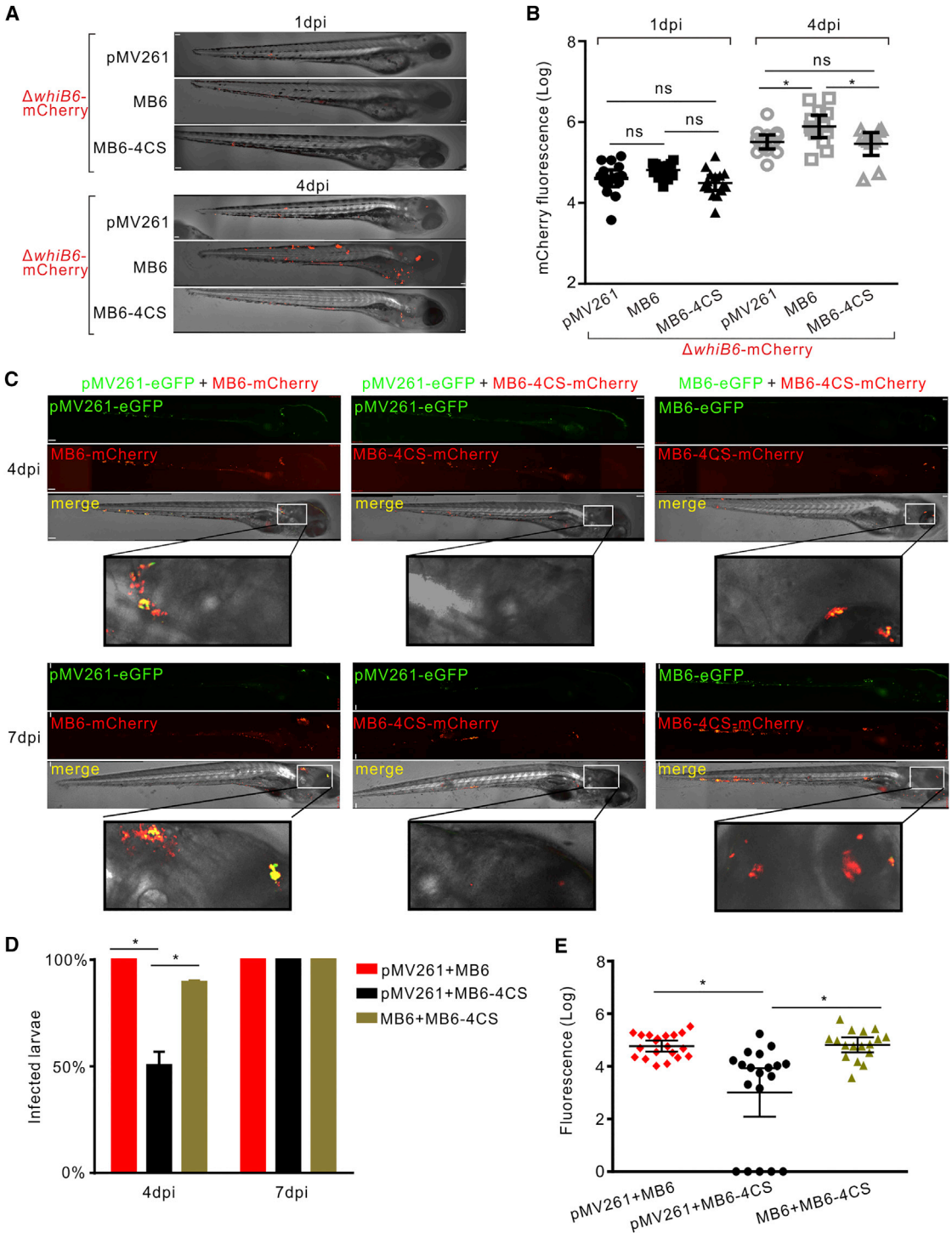

Figure 6. Holo-WhiB6 Accelerates Replication and Spread of *Mm* in Zebrafish Larvae

(A and B) Representative images (A) and mean bacterial burden (B) of zebrafish larvae infected with ~150 cfu fluorescent *Mm* strains via the caudal vein at 1 and 4 dpi. Scale bar, 70 μm (A). Error bars indicate SEM (B).

(C) Representative images of larvae co-infected with ~150 cfu each of two of the fluorescent *Mm* strains via the caudal vein at 4 and 7 dpi. Scale bar, 70 μm.

(D) Percentage of larvae with *Mm* in the brain at 4 and 7 dpi. Data represent the average values from two independent experiments.

(E) Mean fluorescence of larvae co-infected with ~150 cfu each of two of the fluorescent *Mm* strains via the caudal vein at 7 dpi. Error bars indicate SEM of two independent experiments performed in triplicate.

ESX-1. In addition, the ESX-1 virulence locus has been documented to promote both apoptosis of infected macrophages and recruitment of additional macrophages to form the granuloma (Volkman et al., 2004). Thus, the ESX-1 mutant is not likely to induce apoptosis of infected macrophages, and fewer macrophages will need to be recruited, thus reducing the macrophage demand. The ESX-1 mutant produced less necrosis in the granulomas than their WT counterparts in *csf1r* (colony-stimulating factor-1 receptor) mutants, demonstrating that reducing macrophage demand curtails granuloma necrosis by delaying depletion of the macrophages (Pagán et al., 2015). Accordingly, adult zebrafish infected with MB6 or TB6 in which ESX-1 function was strengthened exhibited accelerated granuloma necrosis (Figures 5G and 5J), whereas zebrafish infected with TB6-4CS and MB6-4CS showed delayed necrotic granuloma formation (Figures 5H and 5K). Thus, our findings suggest a mechanism whereby WhiB6 modulates macrophage demand mediated by ESX-1 and then influences the rate of the granuloma's transition to the necrotic phase.

Using both guinea pigs and monkeys, studies have shown that the granulomas are hypoxic and DosR is expressed in the *Mtb* population within these granulomas (Mehra et al., 2015; Via et al., 2008). Unexpectedly, there is a clear overlap between our transcriptional profiling of reduced apo-WhiB6-like complemented *Mm* and the transcriptional profiles of *Mtb* that have been treated with NO (Voskuil et al., 2003) or subjected to oxygen deprivation (Rustad et al., 2008). Our transcriptomic data suggest that reduced apo-WhiB6, unlike holo-WhiB6, stimulates hypoxic stress responses, including the Dos dormancy regulon. Our qRT-PCR results confirmed that mutations of the conserved Cys to Ser in WhiB6, which mimics reduced apo-WhiB6, induced expression of the DosR regulon, while holo-WhiB6 exerts negative regulation (Figures 3B and S3E). Noticeably, holo-WhiB6 induces expression of dormancy-related genes when exposed to NO, but expression of *devH* in the Δ*whiB6*-vec also increased upon 180-min DETA-NO exposure, which is comparable to MB6 and TB6 (Figure 4C). DevH is also upregulated by phosphorylated DevR under hypoxic conditions and NO exposure (Ohno et al., 2003; Rodriguez et al., 2008; Voskuil et al., 2003). Thus, following 30 min and 60 min exposure to DETA-NO, *devH* was also induced in the Δ*whiB6*-vec strain, but its expression was still reduced compared with MB6. When these two strains were exposed to DETA-NO for 180 min, expression of *devH* may reach levels that override the effect of WhiB6 on the DosR regulon. This may explain why *devH* expression in the Δ*whiB6*-vec control increases upon 180-min DETA-NO exposure to levels comparable to that in MB6 and TB6. The reverse regulation of the ESX-1 and the DosR regulons mediated by holo-WhiB6 and WhiB6-DNIC, respectively, reveals the dynamic regulatory role of WhiB6, which has not been reported for other WhiB family members.

Our results suggest that WhiB6 may act as a finely tuned regulator of the ESX-1 secretion system and DosR regulon by its Fe-S cluster in response to NO or O_2. The ESX-1 secretion system is required for acute infection in mice (Stanley et al., 2003), while *dosRS* are required for long-term persistence in macaques (Mehra et al., 2015). Thus, both the ESX-1 secretion system and the *dosRS* regulon are important virulence factors responsible for different phases of infection. Although ESX-1 is downregulated in Δ*whiB6*, the DosR regulon is upregulated, which may explain why Δ*whiB6* has similar survival rates in the zebrafish model compared to the WT strain. Alternatively, the high infection dosage (~5,000 cfu) may also influence the outcome of WT and Δ*whiB6* infected zebrafish (Parikka et al., 2012). Notably, histological analysis of Δ*whiB6* and WT infected zebrafish revealed important differences in granuloma formation at 4 wpi, suggesting that WhiB6 modulates granuloma development and architecture.

It is also noteworthy that there is a significant overlap between the genes regulated in *Mtb* Δ*whiB4* and those differentially expressed in MB6-4CS, including the *iniBAC* operon, *ahpC-aphD*, and *whiB4*, which were all specifically regulated by reduced apo-WhiB6-like isoform, in contrast to holo-WhiB6, which had little effect (Figures 3A and S6B). Coincidently, these genes were differentially expressed in *Mtb* upon exposure to the front-line anti-tuberculosis drug isoniazid (INH) (Karakousis et al., 2008). *katG*, a gene that encodes catalase peroxidase, has been found to be associated with INH resistance in clinical isolates (Zhang et al., 1993) and was also specifically downregulated by the reduced apo-WhiB6-like isoform (Figure S6B). Together, we hypothesized that accumulation of NADH, resulting from unavailability of oxygen during hypoxia, promotes formation of reduced apo-WhiB6 when holo-WhiB6 is largely disrupted upon exposure to oxidative stress. The reduced apo-WhiB6 then differentially reprograms gene expression to induce dormancy and confers INH resistance by downregulating KatG expression (Balaban et al., 2013) and increasing InhA resistance during *Mtb* infection (Larsen et al., 2002).

We propose the following model for the role of WhiB6 (Figure 7): When *Mm* is engulfed by activated macrophages, NO induces the expression of WhiB6, which in turn autoregulates itself to promote ESX-1 to secrete its substrates, which allow *Mm* to survive within the macrophage by phagosomal escape. On the other hand, holo-WhiB6 enhances recruitment of macrophages to the granulomas through ESX-1 and subsequent dissemination of disease (Movies S1 and S3). However, when *Mm* is continually exposed to exogenous reactive oxygen species (ROS) and reactive nitrogen species (RNS) generated by the host immune system, the WhiB6 Fe-S cluster reacts with ROS and NO to generate apo-WhiB6 and a stable DNIC complex, respectively. Increased accumulation of NADH, resulting from the unavailability of oxygen during hypoxia in the granulomas, accelerates reduced apo-WhiB6 formation. Furthermore, reduced apo-WhiB6 may converse to holo-WhiB6 by the cysteine desulfurase IscS (Rv3025c), which is involved in Fe-S cluster biogenesis (Singh et al., 2007). Both WhiB6-DNIC and reduced apo-WhiB6 exert similar effects of transcriptional regulation on *Mtb* that are the reverse of that of holo-WhiB6. These apo-WhiB6 and WhiB6-DNIC regulatory changes will shift metabolism away from aerobic respiration and maintain energy levels and redox balance in *Mm*, mainly via the DosR/S/T dormancy system, which enables *Mm* to establish a persistent infection and maintain the integrity of granulomas (Movies S2 and S4).

EXPERIMENTAL PROCEDURES

Bacterial Strains and Growth Conditions

Strains and plasmids used in this study are summarized in Table S1. Growth conditions are described in the Supplemental Experimental Procedures.

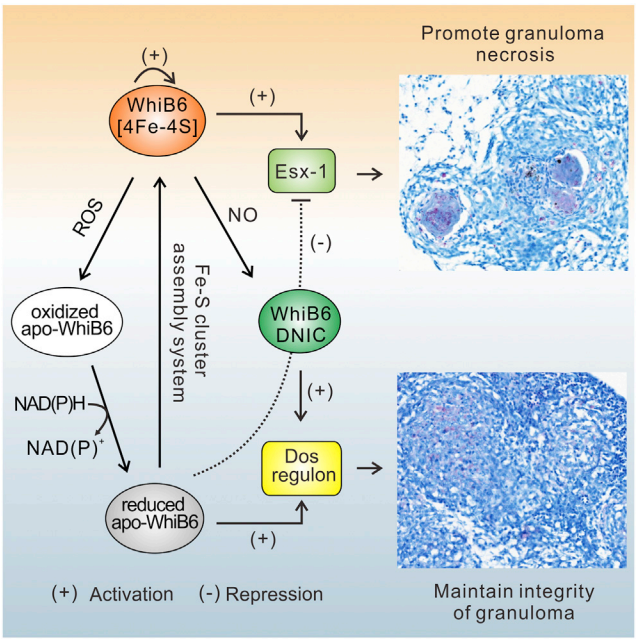

Figure 7. A Model for WhiB6-Mediated Modulation of Disease Dissemination and Maintenance of Granulomas

When *Mm* is phagocytosed by activated macrophages, NO induces expression of *whiB6*. Holo-WhiB6 autoregulates itself to promote ESX-1 expression and consequential secretion of its substrates. Holo-WhiB6 enhances recruitment of macrophages to the granulomas through ESX-1 secreted substrates to promote granuloma necrosis and subsequent dissemination of disease. Yet, when *Mm* is continuously exposed to ROS and RNS produced by the immune system, the WhiB6 Fe-S cluster reacts with ROS and NO to form apo-WhiB6 and WhiB6-DNIC, respectively. Both apo-WhiB6 and WhiB6-DNIC will shift metabolism and maintain energy and redox homeostasis via the DosR regulon, resulting in maintenance of granuloma integrity.

Mm Stress Conditions

The Δ*whiB6*-vec, MB6, and TB6 strains were grown in roller bottles at 32°C in Middlebrook 7H9 liquid medium supplemented with 0.2% glycerol, 0.05% (w/v) Tween-80 and 10% (v/v) Middlebrook oleic acid albumin/dextrose/catalase. When optical density 600 (OD_{600}) reached ~0.4, cells were divided into 30-ml aliquots, returned to incubator for 30 min to equilibrate, and then treated with 300 μM DETA-NO for 30, 60, and 180 min. Cells were harvested by centrifugation, and pellets were frozen in liquid nitrogen and stored at −80°C and used for qRT-PCR as described in Supplemental Experimental Procedures. The same strains were treated with 0, 30, and 300 μM DETA/NO, respectively, for 12 hr, and western blots were performed to detect EsxA and EsxB as described in Supplemental Experimental Procedures.

ChIP Experiments and qRT-PCR Validation

ChIP experiments were performed as described previously (Solans et al., 2014b), with modifications, and are described in the Supplemental Experimental Procedures.

Hemolysis Assay

Contact-dependent hemolysis was assayed as described previously (Gao et al., 2004), with modifications, as described inthe Supplemental Experimental Procedures.

Zebrafish Infection

Zebrafish larvae were obtained from an AB WT or *Tg*(*mpeg1:mCherry*) line (Ellett et al., 2011) (Purchased from China Zebrafish Resource Center) by natural spawning and raised at 28°C in a water tank. Larvae and adult zebrafish infections are described in the Supplemental Experimental Procedures.

Statistical Analysis

Statistical analyses were conducted using GraphPad Prism V6, and values are presented as mean ± SD. The statistical significance of the differences between experimental groups was determined as indicated. p values of less than 0.05 were considered statistically significant.

ACCESSION NUMBERS

The accession number for the sequencing data reported in this paper is SRA: SRP073882.

SUPPLEMENTAL INFORMATION

Supplemental Information includes Supplemental Experimental Procedures, seven figures, three tables, and four movies and can be found with this article online at http://dx.doi.org/10.1016/j.celrep.2016.07.080.

AUTHOR CONTRIBUTIONS

Z.C. and S.C. designed research. Z.C., Y.H., and P.L. performed research. Y.H., L.F., and J.D. contributed reagents and analytic tools. Z.C., B.M.C., A.J.C.S., and S.C. analyzed data and wrote the paper. All authors discussed the results and commented on the manuscript.

ACKNOWLEDGMENTS

We thank Jun Liu for providing *M. marinum* ATCC BAA-535, Yunbing Zhang for expert technical assistance with zebrafish service, Fang Peng for allowing us to use the anaerobic workstation, and the Core Facility and Technical Support of Wuhan Institute of Virology for image collection. The reagents used for genomic DNA of *M. tuberculosis* H37Rv (NR-14865) and anti-EsxB (NR-1380) were obtained through BEI Resources, National Institute of Allergy and Infectious Diseases, NIH. This work was supported by the Key Research Program of the Chinese Academy of Sciences (KJZD-EW-L02) and the National Natural Science Foundation of China (grant no. 81271797).

Received: May 2, 2016
Revised: July 6, 2016
Accepted: July 27, 2016
Published: August 18, 2016

REFERENCES

Abdallah, A.M., Bestebroer, J., Savage, N.D.L., de Punder, K., van Zon, M., Wilson, L., Korbee, C.J., van der Sar, A.M., Ottenhoff, T.H.M., van der Wel, N.N., et al. (2011). Mycobacterial secretion systems ESX-1 and ESX-5 play distinct roles in host cell death and inflammasome activation. J. Immunol. *187*, 4744–4753.

Alam, M.S., Garg, S.K., and Agrawal, P. (2009). Studies on structural and functional divergence among seven WhiB proteins of Mycobacterium tuberculosis H37Rv. FEBS J. *276*, 76–93.

Balaban, N.Q., Gerdes, K., Lewis, K., and McKinney, J.D. (2013). A problem of persistence: still more questions than answers? Nat. Rev. Microbiol. *11*, 587–591.

Boon, C., and Dick, T. (2012). How Mycobacterium tuberculosis goes to sleep: the dormancy survival regulator DosR a decade later. Future Microbiol. *7*, 513–518.

Boshoff, H.I.M., Xu, X., Tahlan, K., Dowd, C.S., Pethe, K., Camacho, L.R., Park, T.-H., Yun, C.-S., Schnappinger, D., Ehrt, S., et al. (2008). Biosynthesis and recycling of nicotinamide cofactors in mycobacterium tuberculosis. An essential role for NAD in nonreplicating bacilli. J. Biol. Chem. *283*, 19329–19341.

Burian, J., Yim, G., Hsing, M., Axerio-Cilies, P., Cherkasov, A., Spiegelman, G.B., and Thompson, C.J. (2013). The mycobacterial antibiotic resistance determinant WhiB7 acts as a transcriptional activator by binding the primary sigma factor SigA (RpoV). Nucleic Acids Res. *41*, 10062–10076.

Cambier, C.J., Falkow, S., and Ramakrishnan, L. (2014). Host evasion and exploitation schemes of Mycobacterium tuberculosis. Cell *159*, 1497–1509.

Casonato, S., Cervantes Sánchez, A., Haruki, H., Rengifo González, M., Provvedi, R., Dainese, E., Jaouen, T., Gola, S., Bini, E., Vicente, M., et al. (2012). WhiB5, a transcriptional regulator that contributes to Mycobacterium tuberculosis virulence and reactivation. Infect. Immun. *80*, 3132–3144.

Champion, M.M., Williams, E.A., Pinapati, R.S., and Champion, P.A.D. (2014). Correlation of phenotypic profiles using targeted proteomics identifies mycobacterial esx-1 substrates. J. Proteome Res. *13*, 5151–5164.

Chan, J., Xing, Y., Magliozzo, R.S., and Bloom, B.R. (1992). Killing of virulent Mycobacterium tuberculosis by reactive nitrogen intermediates produced by activated murine macrophages. J. Exp. Med. *175*, 1111–1122.

Chan, J., Tanaka, K., Carroll, D., Flynn, J., and Bloom, B.R. (1995). Effects of nitric oxide synthase inhibitors on murine infection with Mycobacterium tuberculosis. Infect. Immun. *63*, 736–740.

Chawla, M., Parikh, P., Saxena, A., Munshi, M., Mehta, M., Mai, D., Srivastava, A.K., Narasimhulu, K.V., Redding, K.E., Vashi, N., et al. (2012). Mycobacterium tuberculosis WhiB4 regulates oxidative stress response to modulate survival and dissemination in vivo. Mol. Microbiol. *85*, 1148–1165.

Cumming, B.M., and Steyn, A.J. (2015). Metabolic plasticity of central carbon metabolism protects mycobacteria. Proc. Natl. Acad. Sci. USA *112*, 13135–13136.

Davis, J.M., and Ramakrishnan, L. (2009). The role of the granuloma in expansion and dissemination of early tuberculous infection. Cell *136*, 37–49.

Dutta, N.K., and Karakousis, P.C. (2014). Latent tuberculosis infection: myths, models, and molecular mechanisms. Microbiol. Mol. Biol. Rev. *78*, 343–371.

Ehrt, S., and Schnappinger, D. (2009). Mycobacterial survival strategies in the phagosome: defence against host stresses. Cell. Microbiol. *11*, 1170–1178.

Ellett, F., Pase, L., Hayman, J.W., Andrianopoulos, A., and Lieschke, G.J. (2011). mpeg1 promoter transgenes direct macrophage-lineage expression in zebrafish. Blood *117*, e49–e56.

Flannagan, R.S.C., Cosío, G., and Grinstein, S. (2009). Antimicrobial mechanisms of phagocytes and bacterial evasion strategies. Nat. Rev. Microbiol. *7*, 355–366.

Gao, L.-Y., Guo, S., McLaughlin, B., Morisaki, H., Engel, J.N., and Brown, E.J. (2004). A mycobacterial virulence gene cluster extending RD1 is required for cytolysis, bacterial spreading and ESAT-6 secretion. Mol. Microbiol. *53*, 1677–1693.

Geiman, D.E., Raghunand, T.R., Agarwal, N., and Bishai, W.R. (2006). Differential gene expression in response to exposure to antimycobacterial agents and other stress conditions among seven Mycobacterium tuberculosis whiB-like genes. Antimicrob. Agents Chemother. *50*, 2836–2841.

Gengenbacher, M., and Kaufmann, S.H. (2012). Mycobacterium tuberculosis: success through dormancy. FEMS Microbiol. Rev. *36*, 514–532.

Goodsmith, N., Guo, X.V., Vandal, O.H., Vaubourgeix, J., Wang, R., Botella, H., Song, S., Bhatt, K., Liba, A., Salgame, P., et al. (2015). Disruption of an M. tuberculosis membrane protein causes a magnesium-dependent cell division defect and failure to persist in mice. PLoS Pathog. *11*, e1004645.

Hartman, T., Weinrick, B., Vilchèze, C., Berney, M., Tufariello, J., Cook, G.M., and Jacobs, W.R., Jr. (2014). Succinate dehydrogenase is the regulator of respiration in Mycobacterium tuberculosis. PLoS Pathog. *10*, e1004510.

Homolka, S., Niemann, S., Russell, D.G., and Rohde, K.H. (2010). Functional genetic diversity among Mycobacterium tuberculosis complex clinical isolates: delineation of conserved core and lineage-specific transcriptomes during intracellular survival. PLoS Pathog. *6*, e1000988.

Houben, D., Demangel, C., van Ingen, J., Perez, J., Baldeón, L., Abdallah, A.M., Caleechurn, L., Bottai, D., van Zon, M., de Punder, K., et al. (2012). ESX-1-mediated translocation to the cytosol controls virulence of mycobacteria. Cell. Microbiol. *14*, 1287–1298.

Hurley, J.K., Weber-Main, A.M., Hodges, A.E., Stankovich, M.T., Benning, M.M., Holden, H.M., Cheng, H., Xia, B., Markley, J.L., Genzor, C., et al. (1997). Iron-sulfur cluster cysteine-to-serine mutants of Anabaena -2Fe-2S-ferredoxin exhibit unexpected redox properties and are competent in electron transfer to ferredoxin:NADP+ reductase. Biochemistry *36*, 15109–15117.

Joshi, S.A., Ball, D.A., Sun, M.G., Carlsson, F., Watkins, B.Y., Aggarwal, N., McCracken, J.M., Huynh, K.K., and Brown, E.J. (2012). EccA1, a component of the Mycobacterium marinum ESX-1 protein virulence factor secretion pathway, regulates mycolic acid lipid synthesis. Chem. Biol. *19*, 372–380.

Karakousis, P.C., Williams, E.P., and Bishai, W.R. (2008). Altered expression of isoniazid-regulated genes in drug-treated dormant Mycobacterium tuberculosis. J. Antimicrob. Chemother. *61*, 323–331.

Kassa, D., Ran, L., Geberemeskel, W., Tebeje, M., Alemu, A., Selase, A., Tegbaru, B., Franken, K.L.M.C., Friggen, A.H., van Meijgaarden, K.E., et al. (2012). Analysis of immune responses against a wide range of Mycobacterium tuberculosis antigens in patients with active pulmonary tuberculosis. Clin. Vaccine Immunol. *19*, 1907–1915.

Konar, M., Alam, M.S., Arora, C., and Agrawal, P. (2012). WhiB2/Rv3260c, a cell division-associated protein of Mycobacterium tuberculosis H37Rv, has properties of a chaperone. FEBS J. *279*, 2781–2792.

Kumar, A., Toledo, J.C., Patel, R.P., Lancaster, J.R., Jr., and Steyn, A.J. (2007). Mycobacterium tuberculosis DosS is a redox sensor and DosT is a hypoxia sensor. Proc. Natl. Acad. Sci. USA *104*, 11568–11573.

Kumar, A., Deshane, J.S., Crossman, D.K., Bolisetty, S., Yan, B.-S., Kramnik, I., Agarwal, A., and Steyn, A.J.C. (2008). Heme oxygenase-1-derived carbon monoxide induces the Mycobacterium tuberculosis dormancy regulon. J. Biol. Chem. *283*, 18032–18039.

Langenau, D.M., and Zon, L.I. (2005). The zebrafish: a new model of T-cell and thymic development. Nat. Rev. Immunol. *5*, 307–317.

Larsen, M.H., Vilchèze, C., Kremer, L., Besra, G.S., Parsons, L., Salfinger, M., Heifets, L., Hazbon, M.H., Alland, D., Sacchettini, J.C., and Jacobs, W.R., Jr. (2002). Overexpression of inhA, but not kasA, confers resistance to isoniazid and ethionamide in Mycobacterium smegmatis, M. bovis BCG and M. tuberculosis. Mol. Microbiol. *46*, 453–466.

Larsson, C., Luna, B., Ammerman, N.C., Maiga, M., Agarwal, N., and Bishai, W.R. (2012). Gene expression of Mycobacterium tuberculosis putative transcription factors whiB1-7 in redox environments. PLoS ONE *7*, e37516.

Leistikow, R.L., Morton, R.A., Bartek, I.L., Frimpong, I., Wagner, K., and Voskuil, M.I. (2010). The Mycobacterium tuberculosis DosR regulon assists in metabolic homeostasis and enables rapid recovery from nonrespiring dormancy. J. Bacteriol. *192*, 1662–1670.

McLaughlin, B., Chon, J.S., MacGurn, J.A., Carlsson, F., Cheng, T.L., Cox, J.S., and Brown, E.J. (2007). A mycobacterium ESX-1-secreted virulence factor with unique requirements for export. PLoS Pathog. *3*, e105.

Mehra, S., Foreman, T.W., Didier, P.J., Ahsan, M.H., Hudock, T.A., Kissee, R., Golden, N.A., Gautam, U.S., Johnson, A.-M., Alvarez, X., et al. (2015). The DosR regulon modulates adaptive immunity and is essential for Mycobacterium tuberculosis persistence. Am. J. Respir. Crit. Care Med. *191*, 1185–1196.

Ohno, H., Zhu, G., Mohan, V.P., Chu, D., Kohno, S., Jacobs, W.R., Jr., and Chan, J. (2003). The effects of reactive nitrogen intermediates on gene expression in Mycobacterium tuberculosis. Cell. Microbiol. *5*, 637–648.

Pagán, A.J., and Ramakrishnan, L. (2014). Immunity and immunopathology in the tuberculous granuloma. Cold Spring Harb. Perspect. Med. *5*, a018499.

Pagán, A.J., Yang, C.-T., Cameron, J., Swaim, L.E., Ellett, F., Lieschke, G.J., and Ramakrishnan, L. (2015). Myeloid growth factors promote resistance to Mycobacterial infection by curtailing granuloma necrosis through macrophage replenishment. Cell Host Microbe *18*, 15–26.

Parikka, M., Hammarén, M.M., Harjula, S.K., Halfpenny, N.J., Oksanen, K.E., Lahtinen, M.J., Pajula, E.T., Iivanainen, A., Pesu, M., and Rämet, M. (2012). Mycobacterium marinum causes a latent infection that can be reactivated by gamma irradiation in adult zebrafish. PLoS Pathog. *8*, e1002944.

Philips, J.A., and Ernst, J.D. (2012). Tuberculosis pathogenesis and immunity. Annu. Rev. Pathol. *7*, 353–384.

Ramakrishnan, L. (2012). Revisiting the role of the granuloma in tuberculosis. Nat. Rev. Immunol. *12*, 352–366.

Rao, S.P.S., Alonso, S., Rand, L., Dick, T., and Pethe, K. (2008). The protonmotive force is required for maintaining ATP homeostasis and viability of hypoxic, nonreplicating Mycobacterium tuberculosis. Proc. Natl. Acad. Sci. USA *105*, 11945–11950.

Rodriguez, J.G., Burbano, C.S., Nuñez, C., González, C.E., Zambrano, M.M., García, M.J., and Del Portillo, P. (2008). Rv3134c/devR/devS operon of Mycobacterium bovis BCG is differentially transcribed under "in vitro" stress conditions. Tuberculosis (Edinb.) *88*, 273–282.

Rustad, T.R., Harrell, M.I., Liao, R., and Sherman, D.R. (2008). The enduring hypoxic response of Mycobacterium tuberculosis. PLoS ONE *3*, e1502.

Rustad, T.R., Sherrid, A.M., Minch, K.J., and Sherman, D.R. (2009). Hypoxia: a window into Mycobacterium tuberculosis latency. Cell. Microbiol. *11*, 1151–1159.

Saini, V., Farhana, A., Glasgow, J.N., and Steyn, A.J.C. (2012a). Iron sulfur cluster proteins and microbial regulation: implications for understanding tuberculosis. Curr. Opin. Chem. Biol. *16*, 45–53.

Saini, V., Farhana, A., and Steyn, A.J.C. (2012b). Mycobacterium tuberculosis WhiB3: a novel iron-sulfur cluster protein that regulates redox homeostasis and virulence. Antioxid. Redox Signal. *16*, 687–697.

Schnappinger, D., Ehrt, S., Voskuil, M.I., Liu, Y., Mangan, J.A., Monahan, I.M., Dolganov, G., Efron, B., Butcher, P.D., Nathan, C., and Schoolnik, G.K. (2003). Transcriptional adaptation of Mycobacterium tuberculosis within macrophages: insights into the phagosomal environment. J. Exp. Med. *198*, 693–704.

Shiloh, M.U., Manzanillo, P., and Cox, J.S. (2008). Mycobacterium tuberculosis senses host-derived carbon monoxide during macrophage infection. Cell Host Microbe *3*, 323–330.

Simeone, R., Bobard, A., Lippmann, J., Bitter, W., Majlessi, L., Brosch, R., and Enninga, J. (2012). Phagosomal rupture by Mycobacterium tuberculosis results in toxicity and host cell death. PLoS Pathog. *8*, e1002507.

Singh, A., Guidry, L., Narasimhulu, K.V., Mai, D., Trombley, J., Redding, K.E., Giles, G.I., Lancaster, J.R., Jr., and Steyn, A.J. (2007). Mycobacterium tuberculosis WhiB3 responds to O2 and nitric oxide via its [4Fe-4S] cluster and is essential for nutrient starvation survival. Proc. Natl. Acad. Sci. USA *104*, 11562–11567.

Singh, A., Crossman, D.K., Mai, D., Guidry, L., Voskuil, M.I., Renfrow, M.B., and Steyn, A.J.C. (2009). Mycobacterium tuberculosis WhiB3 maintains redox homeostasis by regulating virulence lipid anabolism to modulate macrophage response. PLoS Pathog. *5*, e1000545.

Smith, L.J., Stapleton, M.R., Fullstone, G.J., Crack, J.C., Thomson, A.J., Le Brun, N.E., Hunt, D.M., Harvey, E., Adinolfi, S., Buxton, R.S., and Green, J. (2010). Mycobacterium tuberculosis WhiB1 is an essential DNA-binding protein with a nitric oxide-sensitive iron-sulfur cluster. Biochem. J. *432*, 417–427.

Solans, L., Aguiló, N., Samper, S., Pawlik, A., Frigui, W., Martín, C., Brosch, R., and Gonzalo-Asensio, J. (2014a). A specific polymorphism in Mycobacterium tuberculosis H37Rv causes differential ESAT-6 expression and identifies WhiB6 as a novel ESX-1 component. Infect. Immun. *82*, 3446–3456.

Solans, L., Gonzalo-Asensio, J., Sala, C., Benjak, A., Uplekar, S., Rougemont, J., Guilhot, C., Malaga, W., Martín, C., and Cole, S.T. (2014b). The PhoP-dependent ncRNA Mcr7 modulates the TAT secretion system in Mycobacterium tuberculosis. PLoS Pathog. *10*, e1004183.

Spiro, S. (2007). Regulators of bacterial responses to nitric oxide. FEMS Microbiol. Rev. *31*, 193–211.

Stanley, S.A., Raghavan, S., Hwang, W.W., and Cox, J.S. (2003). Acute infection and macrophage subversion by Mycobacterium tuberculosis require a specialized secretion system. Proc. Natl. Acad. Sci. USA *100*, 13001–13006.

Tobin, D.M., Vary, J.C., Jr., Ray, J.P., Walsh, G.S., Dunstan, S.J., Bang, N.D., Hagge, D.A., Khadge, S., King, M.-C., Hawn, T.R., et al. (2010). The lta4h locus modulates susceptibility to mycobacterial infection in zebrafish and humans. Cell *140*, 717–730.

Via, L.E., Lin, P.L., Ray, S.M., Carrillo, J., Allen, S.S., Eum, S.Y., Taylor, K., Klein, E., Manjunatha, U., Gonzales, J., et al. (2008). Tuberculous granulomas are hypoxic in guinea pigs, rabbits, and nonhuman primates. Infect. Immun. *76*, 2333–2340.

Volkman, H.E., Clay, H., Beery, D., Chang, J.C.W., Sherman, D.R., and Ramakrishnan, L. (2004). Tuberculous granuloma formation is enhanced by a mycobacterium virulence determinant. PLoS Biol. *2*, e367.

Voskuil, M.I., Schnappinger, D., Visconti, K.C., Harrell, M.I., Dolganov, G.M., Sherman, D.R., and Schoolnik, G.K. (2003). Inhibition of respiration by nitric oxide induces a Mycobacterium tuberculosis dormancy program. J. Exp. Med. *198*, 705–713.

Zhang, Y., Garbe, T., and Young, D. (1993). Transformation with katG restores isoniazid-sensitivity in Mycobacterium tuberculosis isolates resistant to a range of drug concentrations. Mol. Microbiol. *8*, 521–524.